HHS Public Access

Author manuscript

Biochemistry. Author manuscript; available in PMC 2021 January 01.

Published in final edited form as:

Biochemistry. 2016 August 02; 55(30): 4135–4139. doi:10.1021/acs.biochem.6b00626.

Crystal structures of the iron-sulfur cluster dependent quinolinate synthase in complex with dihydroxyacetone phosphate, iminoaspartate analogs, and quinolinate

Michael K. Fenwick, **Steven E. Ealick***

Department of Chemistry and Chemical Biology, Cornell University, Ithaca, New York 14853, United States

Abstract

The quinolinate synthase of prokaryotes and photosynthetic eukaryotes, NadA, contains a [4Fe-4S] cluster with unknown function. We report crystal structures of *Pyrococcus horikoshii* NadA in complex with dihydroxyacetone phosphate (DHAP), iminoaspartate analogs, and quinolinate. DHAP adopts a nearly planar conformation and chelates the [4Fe-4S] cluster via its keto and hydroxyl groups. The active-site architecture suggests that the cluster acts as a Lewis acid in enediolate formation, similar to zinc in class II aldolases. The DHAP and putative iminoaspartate structures suggest a model for a condensed intermediate. The ensemble of structures suggests a two-state system, which may be exploited in early steps.

Graphical Abstract

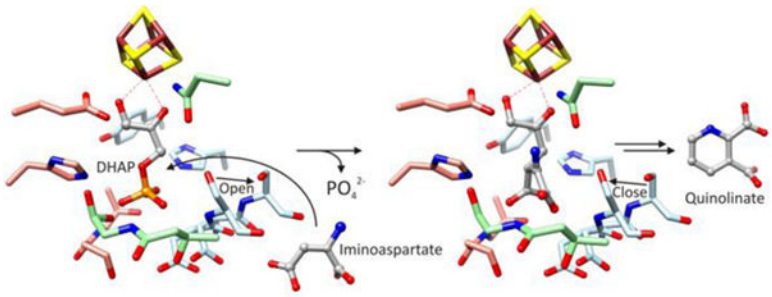

De novo biosynthesis of nicotinamide adenine dinucleotide (NAD) occurs via the intermediate quinolinate (QA) for which two major biosynthetic pathways are known.[1,2] The pathway used by most bacteria, plants, and algae starts from L-aspartate and requires two enzymes, flavin adenine dinucleotide (FAD) dependent L-aspartate oxidase, NadB,[3] and [4Fe-4S] cluster dependent QA synthase, NadA.[4–6] In some organisms, NadB is replaced by

***Corresponding Author** see3@cornell.edu. Telephone: (607) 255-7961.

ASSOCIATED CONTENT

Supporting Information

Materials and Methods, Tables S1-S3, and Figures S1-S8. (PDF)

The coordinates of *Ph*NadA (5KTM), *Ph*NadA/DHAP (5KTN), *Ph*NadA/quinolinate (5KTO), *Ph*NadA/itaconate (5KTP), *Ph*NadA/maleate (5KTR), *Ph*NadA/citraconate (5KTS), and *Ph*NadA/L-malate (5KTT) have been deposited in the Protein Data Bank.

The authors declare no competing financial interests.

NAD(P) dependent L-aspartate dehydrogenase.[7] NadB catalyzes the oxidation of L-aspartate to iminoaspartate (IA) via reduction of FAD to $FADH_2$[3,8,9] and structural studies suggest an enamine product.[10] NadA catalyzes two condensations to form the pyridine ring of QA from IA and dihydroxyacetone phosphate (DHAP), eliminating phosphate and two waters (Scheme 1).[3,11]

Labeling studies showed that the pyridine C_4 originates from C_1 of DHAP, indicating the mode of condensation.[12] Two mechanisms have been proposed.[1,3] Both start with DHAP and require a keto-aldo isomerization that precedes Schiff base formation between the imine nitrogen of IA and C_3 of DHAP. Nasu et al. proposed that these steps occur after C_1-C_β bond formation and phosphate elimination (Fig. S1A),[3] whereas Begley et al. proposed that ketose-aldose isomerization occurs at the outset, producing glyceraldehyde 3-phosphate (G3P) and allowing the Schiff base to form first (Fig. S1B).[1] Biochemical studies suggest that DHAP rather than G3P condenses with IA.[11,13] However, little is known about the mechanism and the role of the [4Fe-4S] cluster.

Crystal structures have been reported for *Pyrococcus horikoshii* NadA (*Ph*NadA),[14] *Pyrococcoccus furiosus* NadA (*Pf*NadA),[15] and *Thermotoga maritima* NadA (*Tm*NadA).[16] The first structure of *Ph*NadA showed a triangular monomer containing three domains and a bound malate identified the active site. However, the structure lacked a [4Fe-4S] cluster.[14] The structure of *Pf*NadA displayed an alternate domain arrangement and oligomeric state, but also lacked a [4Fe-4S] cluster.[15] The structure of *Tm*NadA, reported recently, revealed the location of the [4Fe-4S] cluster and identified a charge relay system.[16] Finally, a second structure of *Ph*NadA, also reported recently, showed a [4Fe-4S] cluster with bound QA.[17]

Here, we report high-resolution crystal structures of *Ph*NadA with a bound [4Fe-4S] cluster and with bound DHAP, itaconate (IA analog), maleate, citraconate (enamine **4** analogs), and L-malate (L-aspartate analog). We also report a high-resolution crystal structure of *Ph*NadA with bound QA. *Ph*NadA was prepared with a [4Fe-4S] cluster by coexpression with the *Escherichia coli suf* operon using *E. coli* BL21 (DE3) as the host strain.[18,19] Purification and crystallization were performed in an anaerobic chamber. Crystals were irradiated at beam lines NE-CAT 24-ID-E of the Advanced Photon Source (APS) and A1 and F1 of the Cornell High Energy Synchrotron Source (CHESS). The structure of *Ph*NadA lacking a [4Fe-4S] cluster[14] was used as a search model for molecular replacement. COOT,[20] PHENIX,[21] and CHIMERA[22] were used for model building, refinement, and analysis. Difference electron density for the ligands is shown in Fig. S2 and data collection and refinement statistics are given in Tables S1-S3.

*Ph*NadA contains three domains displaying pseudo three-fold symmetry that each contribute a cysteine residue for ligation to a centrally located [4Fe-4S] cluster (Fig. S3A-C). The overall structure resembles that of the enzymes IspH and Dph2.[15] Each cysteine thiolate resides at the positive end of a 5-residue helix (Fig. S3D). IspH contains a similar cluster-binding motif except the helices are ~3 times longer.[23] In contrast, Dph2 positions one of the thiolates near the positive end of a short helix; the other two reside in short turns.[24]

DHAP binds the unique (unligated) iron of the [4Fe-4S] cluster via its keto and hydroxyl groups and forms several hydrogen bonds with *Ph*NadA via its phosphate (Fig. 1A). The conformation of DHAP is nearly planar having O_2–C_2–C_3–O_3, C_1–C_2–C_3–O_3, O_1–C_1–C_2–C_3, and O_1–C_1–C_2–O_2 torsional angles of −14.2°, −179.7°, −14.8°, and 179.6°, respectively. O_3 is 2.6 Å from the carboxylate of Glu198 and sp^3 geometry at C_3 places the proR and proS protons near the hydroxyl of Tyr23 and the carboxylate of Glu198, respectively. O_2 is 3.8 Å from the side chain NH_2 of Asn111. The phosphate group is within hydrogen bonding distance of $N_{\varepsilon 2}$ of His21 and His196, the hydroxyl group of Ser38, Ser126, and Thr213, and the backbone NH of Ser38 and Thr213, and may also be stabilized by helix dipoles.

Itaconate is synclinal and occupies the DHAP phosphate site; two waters bind near the [4Fe-4S] cluster (Fig. 1B). The C_1 carboxylate forms hydrogen bonds with the backbone NH of Ser38 and Ser126 and with the hydroxyl of Tyr109; the Cγ carboxylate forms hydrogen bonds with the hydroxyl and backbone NH of Thr213 and with $N_{\varepsilon 2}$ of His21 and His196. The methylene points toward the hydroxyl of Tyr109 and the carboxylate of Glu198.

QA chelates the unique iron of the [4Fe-4S] cluster via its pyridine nitrogen and the carboxylate at C_2, which is also within hydrogen bonding distance of the hydroxyl of Ser38 and Tyr109 (Fig. 1C and Ref. [17]). The carboxylate at C_3 forms hydrogen bonds with $N_{\varepsilon 2}$ of His21 and with the backbone NH of Ser38. The binding mode is similar to that reported recently;[17] however, in our structure chloride binds 3.2 Å from $N_{\varepsilon 2}$ of His196 and the backbone NH of Thr213, and Asn111 and Tyr109 are oriented differently.

Maleate and citraconate bind similar to itaconate but adopt a more planar conformation consistent with a double bond between C_2 and C_3 (Fig. S4A and B). L-malate shows a unique binding mode in which the C_4 carboxylate binds to the unique iron of the [4Fe-4S] cluster and no interactions are made with helix H3 (Fig. S4C). This leads to conformational changes that result in a more open active site cavity, similar to the holoenzyme structure. The ensemble of *Ph*NadA structures suggests a two-state system (Fig. 2).

The structure of DHAP and the nearby architecture support an electrophilic role for the [4Fe-4S] cluster in enediolate formation with phosphate elimination disfavored prior to ternary complex formation. O_3, C_3, C_2, O_2, and C_1 are nearly coplanar, consistent with an enediol(ate)-like structure, and the binding mode is strikingly similar to the mode of binding of phosphoglycolohydroxamate (PGH) to zinc in fuculose-1-phosphate aldolase [25] (FucA) (Fig. 3A). PGH is a *cis* enediolate analog used in studies of triose phosphate isomerase (TPI),[26–28] methylglyoxal synthase (MGS),[29] and class II aldolases,[25,30] which form an enediolate from DHAP via polarization of the C_2 carbonyl, proton abstraction from C_3, and stabilization of the negative charge acquired by O_2. TPI uses a histidine and lysine residue[26,27,31–33] for electrophilic catalysis whereas class II aldolases use zinc;[25,30,34] Fig. 3A suggests that a [4Fe-4S] cluster could play a similar role as zinc. The side chain NH_2 of Asn111 in *Ph*NadA is also well positioned to contribute to O_2 oxyanion stabilization and assist DHAP binding.[26,35,36] TPI and FucA utilize a glutamate residue as the catalytic base[26,37] whereas MGS utilizes an aspartate residue.[38] The side chains of Tyr23 and Glu198 in *Ph*NadA, which are part of a predicted charge relay system and essential for activity,[16,17] are well positioned to perform proton abstractions from C_3 or the C_3 hydroxyl.

Biochemically, an enediol(ate) links intermediates **5** and **6** and may account for the TPI activity reported for NadA in the absence of IA (Fig. S5).[13] The O_1-C_1 bond is “in-plane”, which stereoelectronically disfavors the elimination of phosphate from the enediolate.[25,34,39] Phosphate elimination is likely suppressed further initially by the conformational changes that close the active site cavity in around the bound DHAP (Fig. 2), similar to the role of a mobile loop in TPI, the absence of which accelerates degradative loss of phosphate leading to methylglyoxal.[40] The planarity of the O_1-C_1-C_2-O_2 torsion (~180°) raises the possibility of conjugation.

The bound IA analogs clash severely with the DHAP phosphate (Fig. S6), requiring structural changes for ternary complex formation and phosphate elimination. The nature of these changes and the timing of phosphate elimination are unknown; however, the open state (Fig. 2) is likely required to provide the space needed for binding both substrates and to create an opening for ejecting phosphate. Helix H3 forms a portion of the phosphate-binding site (Fig. 1A) and its conformation depends on the liganded state (Fig. 2). Its conformation in the holo and L-malate bound structures, which is also a minor conformation in the itaconate bound structure, yields an open cavity from which phosphate can be eliminated from an orthogonal conformation (Fig. S7).

After phosphate is eliminated, the closed active site cavity neatly accommodates intermediate **5** and structurally similar intermediates (Fig. S1A). Itaconate, maleate, and citraconate adopt a similar conformation that is also adopted by malate in the absence of the [4Fe-4S] cluster.[14] The conformation is stabilized by several hydrogen bonds and possibly by helix dipoles, suggesting that it is likely adopted by the IA moiety at some point along the reaction coordinate. Superimposition of the [4Fe-4S] cluster with bound DHAP onto the [4Fe-4S] cluster in the itaconate bound structure places the keto and hydroxyl groups by the two waters near the cluster and, without the phosphate, leads to geometry at the C_1-C_β bond consistent with intermediate **5**: C_1 and C_β are 1.67 Å apart with C_1-C_β-C_α and C_1-C_β-C_γ angles of 108.6° and 133.0°, respectively (Fig. 3B). An energy-minimized model is given in Fig. 3C.

The pyridine nitrogen and the adjacent carboxylate in QA chelate the [4Fe-4S] cluster similar to the way the amino and carboxylate groups of S-adenosylmethionine bind a [4Fe-4S] cluster in radical SAM enzymes.[17,41,42] From one point of view, the orientation of QA places C_4 and hydroxylated C_5 of intermediate **8** between the side chains of the essential residues Glu198 and Tyr23, suggesting a potential catalytic role (Fig. 1C). However, the reactions forming intermediate **8** and QA likely do not require enzyme catalysis.[3] This suggests a simpler interpretation of QA formation from transitions between a two-state system starting from bound DHAP activated by the [4Fe-4S] cluster: a closed-to-open cavity transition allowing ternary complex formation, condensation, and phosphate elimination, and an open-to-closed cavity transition stabilizing a later intermediate associated with [4Fe-4S] cluster dependent keto-aldo isomerization.

Supplementary Material

Refer to Web version on PubMed Central for supplementary material.

ACKNOWLEDGMENT

We thank Dr. Tadhg Begley and Dr. Angad Mehta for stimulating discussions, and Dr. Cynthia Kinsland for cloning *Ph*NadA.

Funding Sources

This work is based upon research conducted at the APS on the NE-CAT beamlines, which are supported by award GM103403 from the NIH. Use of the APS is supported by the U.S. Department of Energy, under Contract No. DE-AC02-06CH11357. MacCHESS is supported by NIH grant GM103485 at the CHESS.

REFERENCES

(1). Begley TP, Kinsland C, Mehl RA, Osterman A, and Dorrestein P. (2001), Vitam. Horm 61, 103–119. [PubMed: 11153263]

(2). Gazzaniga F, Stebbins R, Chang SZ, McPeek MA, and Brenner C. (2009), Microbiol. Mol. Biol. Rev 73, 529–541. [PubMed: 19721089]

(3). Nasu S, Wicks FD, and Gholson RK (1982), J. Biol. Chem 257, 626–632. [PubMed: 7033218]

(4). Cicchillo RM, Tu L, Stromberg JA, Hoffart LM, Krebs C, and Booker SJ (2005), J. Am. Chem. Soc 127, 7310–7311. [PubMed: 15898769]

(5). Gardner PR, and Fridovich I. (1991), Arch. Biochem. Biophys 284, 106–111. [PubMed: 1846509]

(6). Ollagnier-de Choudens S, Loiseau L, Sanakis Y, Barras F, and Fontecave M. (2005), FEBS Lett. 579, 3737–3743. [PubMed: 15967443]

(7). Yang Z, Savchenko A, Yakunin A, Zhang R, Edwards A, Arrowsmith C, and Tong L. (2003), J. Biol. Chem 278, 8804–8808. [PubMed: 12496312]

(8). Seifert J, Kunz N, Flachmann R, Laufer A, Jany KD, and Gassen HG (1990), Biol. Chem. Hoppe Seyler 371, 239–248.

(9). Tedeschi G, Negri A, Mortarino M, Ceciliani F, Simonic T, Faotto L, and Ronchi S. (1996), Eur. J. Biochem 239, 427–433. [PubMed: 8706750]

(10). Bossi RT, Negri A, Tedeschi G, and Mattevi A. (2002), Biochemistry 41, 3018–3024. [PubMed: 11863440]

(11). Suzuki N, Carlson J, Griffith G, and Gholson RK (1973), Biochim. Biophys. Acta 304, 309–315. [PubMed: 4351074]

(12). Wicks FD, Sakakibara S, Gholson RK, and Scott TA (1977), Biochim. Biophys. Acta 500, 213–216. [PubMed: 336100]

(13). Reichmann D, Coute Y, and Ollagnier de Choudens S. (2015), Biochemistry 54, 6443–6446. [PubMed: 26455817]

(14). Sakuraba H, Tsuge H, Yoneda K, Katunuma N, and Ohshima T. (2005), J. Biol. Chem 280, 26645–26648. [PubMed: 15937336]

(15). Soriano EV, Zhang Y, Colabroy KL, Sanders JM, Settembre EC, Dorrestein PC, Begley TP, and Ealick SE (2013), Acta Crystallogr. D Biol. Crystallogr 69, 1685–1696. [PubMed: 23999292]

(16). Cherrier MV, Chan A, Darnault C, Reichmann D, Amara P, Ollagnier de Choudens S, and Fontecilla-Camps JC (2014), J. Am. Chem. Soc 136, 5253–5256. [PubMed: 24650327]

(17). Esakova OA, Silakov A, Grove TL, Saunders AH, McLaughlin MI, Yennawar NH, and Booker SJ (2016), J. Am. Chem. Soc 138, 7224–7227. [PubMed: 27224840]

(18). Hanzelmann P, Hernandez HL, Menzel C, Garcia-Serres R, Huynh BH, Johnson MK, Mendel RR, and Schindelin H. (2004), J. Biol. Chem 279, 34721–34732. [PubMed: 15180982]

(19). Mehta AP, Abdelwahed SH, Fenwick MK, Hazra AB, Taga ME, Zhang Y, Ealick SE, and Begley TP (2015), J. Am. Chem. Soc 137, 10444–10447. [PubMed: 26237670]

(20). Emsley P, Lohkamp B, Scott WG, and Cowtan K. (2010), Acta Crystallogr. D66, 486–501.

(21). Adams PD, Afonine PV, Bunkoczi G, Chen VB, Davis IW, Echols N, Headd JJ, Hung LW, Kapral GJ, Grosse-Kunstleve RW, McCoy AJ, Moriarty NW, Oeffner R, Read RJ, Richardson DC, Richardson JS, Terwilliger TC, and Zwart PH (2010), Acta Crystallogr. D Biol. Crystallogr 66, 213–221. [PubMed: 20124702]

(22). Pettersen EF, Goddard TD, Huang CC, Couch GS, Greenblatt DM, Meng EC, and Ferrin TE (2004), J. Comput. Chem 25, 1605–1612. [PubMed: 15264254]

(23). Rekittke I, Wiesner J, Rohrich R, Demmer U, Warkentin E, Xu W, Troschke K, Hintz M, No JH, Duin EC, Oldfield E, Jomaa H, and Ermler U. (2008), J. Am. Chem. Soc 130, 17206–17207. [PubMed: 19035630]

(24). Zhang Y, Zhu X, Torelli AT, Lee M, Dzikovski B, Koralewski RM, Wang E, Freed J, Krebs C, Ealick SE, and Lin H. (2010), Nature 465, 891–896. [PubMed: 20559380]

(25). Dreyer MK, and Schulz GE (1996), J. Mol. Biol 259, 458–466. [PubMed: 8676381]

(26). Davenport RC, Bash PA, Seaton BA, Karplus M, Petsko GA, and Ringe D. (1991), Biochemistry 30, 5821–5826. [PubMed: 2043623]

(27). Komives EA, Chang LC, Lolis E, Tilton RF, Petsko GA, and Knowles JR (1991), Biochemistry 30, 3011–3019. [PubMed: 2007138]

(28). Noble ME, Zeelen JP, and Wierenga RK (1993), Proteins 16, 311–326. [PubMed: 8356028]

(29). Marks GT, Harris TK, Massiah MA, Mildvan AS, and Harrison DH (2001), Biochemistry 40, 6805–6818. [PubMed: 11389594]

(30). Hall DR, Leonard GA, Reed CD, Watt CI, Berry A, and Hunter WN (1999), J. Mol. Biol 287, 383–394. [PubMed: 10080900]

(31). Go MK, Koudelka A, Amyes TL, and Richard JP (2010), Biochemistry 49, 5377–5389. [PubMed: 20481463]

(32). Jogl G, Rozovsky S, McDermott AE, and Tong L. (2003), Proc. Natl. Acad. Sci. U. S. A 100, 50–55. [PubMed: 12509510]

(33). Lodi PJ, and Knowles JR (1991), Biochemistry 30, 6948–6956. [PubMed: 2069953]

(34). Fessner W-D, Schneider A, Held H, Sinerius G, Walter C, Hixon M, and Schloss JV (1996), Angew. Chem. Int. Ed. Engl 35, 2219–2221.

(35). Kursula I, Partanen S, Lambeir AM, Antonov DM, Augustyns K, and Wierenga RK (2001), Eur. J. Biochem 268, 5189–5196. [PubMed: 11589711]

(36). Plater AR, Zgiby SM, Thomson GJ, Qamar S, Wharton CW, and Berry A. (1999), J. Mol. Biol 285, 843–855. [PubMed: 9878448]

(37). Joerger AC, Gosse C, Fessner WD, and Schulz GE (2000), Biochemistry 39, 6033–6041. [PubMed: 10821675]

(38). Saadat D, and Harrison DH (1999), Structure 7, 309–317. [PubMed: 10368300]

(39). Lolis E, and Petsko GA (1990), Biochemistry 29, 6619–6625. [PubMed: 2204418]

(40). Pompliano DL, Peyman A, and Knowles JR (1990), Biochemistry 29, 3186–3194. [PubMed: 2185832]

(41). Layer G, Moser J, Heinz DW, Jahn D, and Schubert WD (2003), EMBO J. 22, 6214–6224. [PubMed: 14633981]

(42). Walsby CJ, Ortillo D, Broderick WE, Broderick JB, and Hoffman BM (2002), J. Am. Chem. Soc 124, 11270–11271. [PubMed: 12236732]

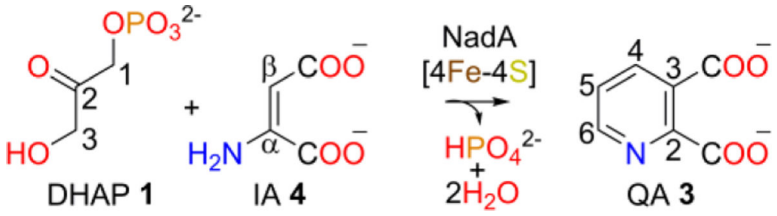

Scheme 1.
NadA catalyzed reaction.

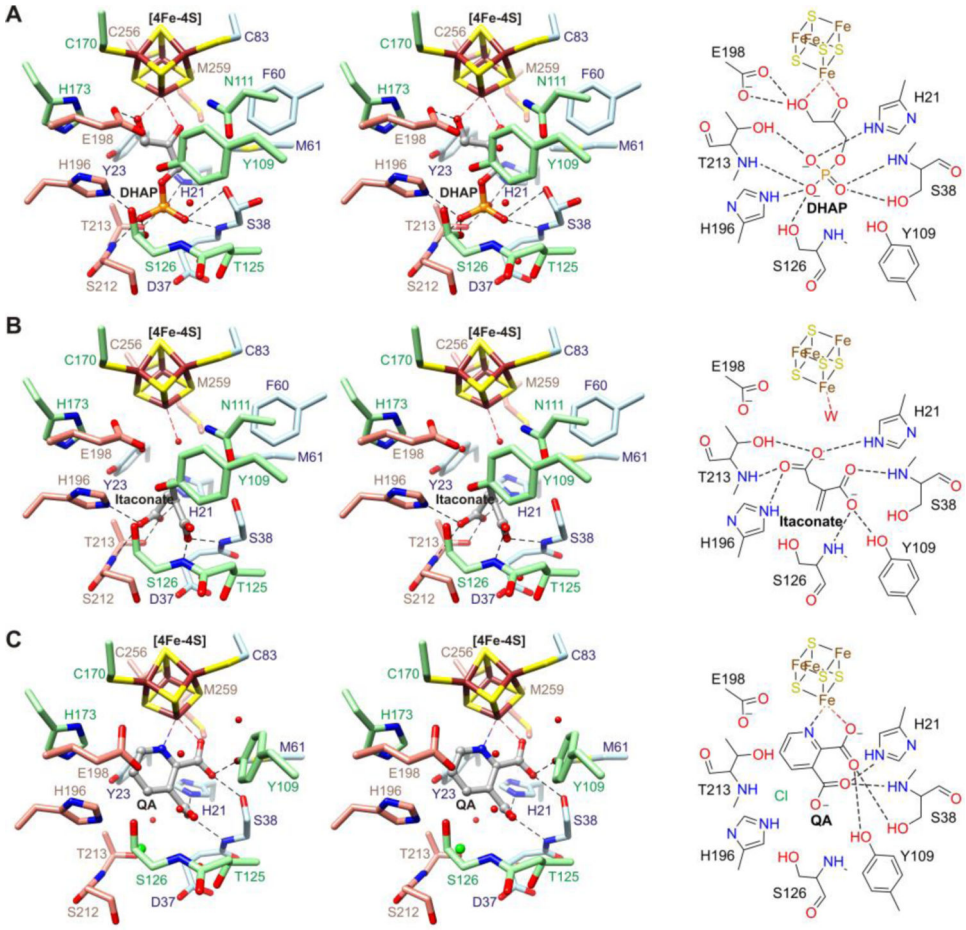

Figure 1.

Stereo diagrams (left) and schematic drawings (right) of the active site of *Ph*NadA with bound (A) DHAP, (B) itaconate, and (C) QA. Black broken lines denote potential hydrogen bonds, red spheres denote waters, and the green sphere denotes chloride.

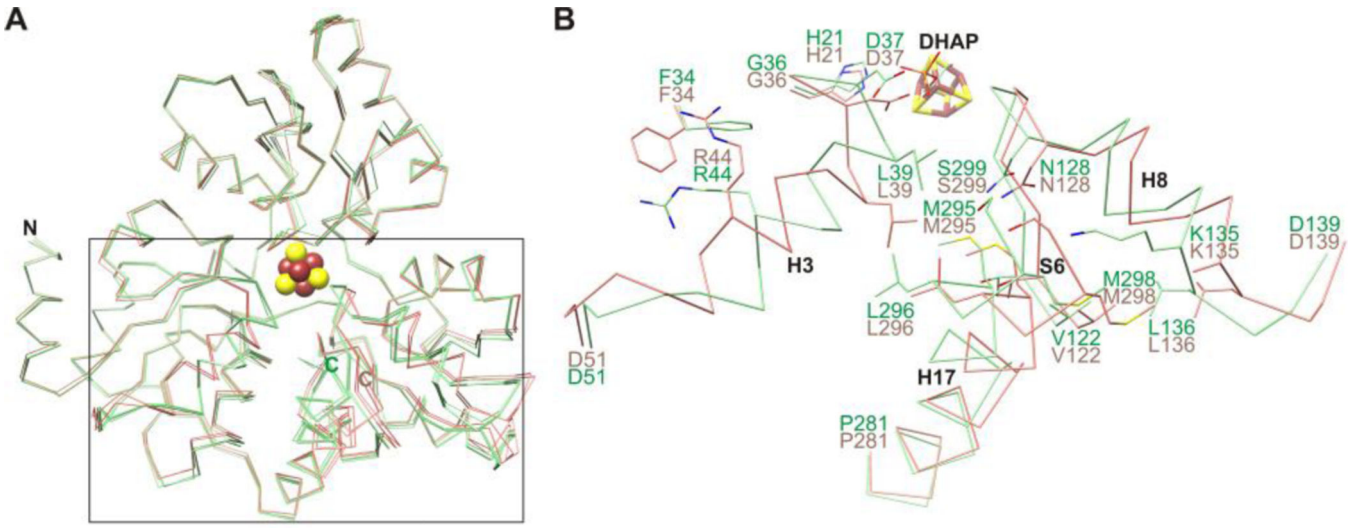

Figure 2.

(A) Superimposition of C_α traces showing open (holo and L-malate bound structures; salmon) and closed (DHAP, itaconate, maleate, and citraconate bound structures; light green) states of *Ph*NadA. (B) Close-up of holo and DHAP bound structures indicating side chain clashes.

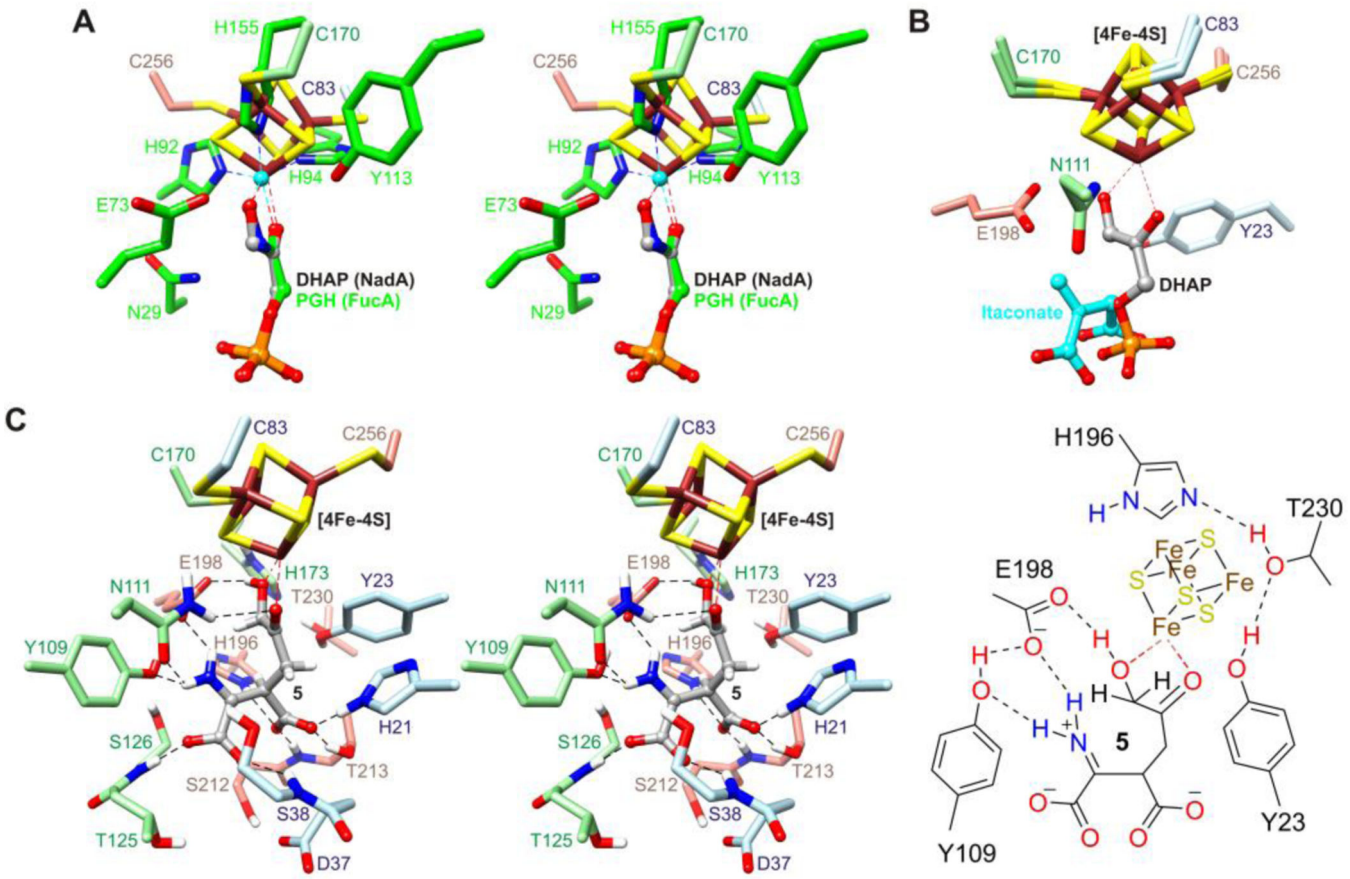

Figure 3.

(A) Stereo diagram of the superimposition of DHAP bound to the [4Fe-4S] cluster in *Ph*NadA onto PGH bound to zinc (cyan) in FucA (green). (B) Superimposition of the [4Fe-4S] cluster with bound DHAP onto the [4Fe-4S] cluster in the itaconate bound structure of *Ph*NadA. (C) Stereo diagram (left) and schematic drawing (right) of intermediate **5** based on the result in panel B, with C_1 and C_β joined, followed by energy minimization with positional restraints applied to the protein atoms.